Reliability-Based Assessment of Damaged Prestressed Concrete I-Girder Bridges

Gianmarco Addonizio, Daniele Losanno

University of Naples Federico II, Naples, IT

Eva O.L. Lantsoght

Delft University of Technology, Delft, NL

Universidad San Francisco de Quito, Quito, EC

Joan R. Casas

UPC-Barcelona-Tech, Barcelona, ES

Contact: gianmarco.addonizio@unina.it

Abstract

Structural assessment of existing bridges becomes a challenging process in the presence of deterioration phenomena and outdated design action and resistance models. This paper explores the potentiality and effectiveness of reliability-based methods in the structural evaluation of existing PC I-girder bridges, highlighting scenarios where conventional methods, such as Partial Safety Factor Method, may underestimate structural capacity. Based on detailed visual inspection, in-situ data of deterioration phenomena is introduced in the probabilistic analysis and a Eurocode-based traffic model is adopted for the traffic load effect characterization. A case study is discussed emphasizing the advantages of adopting a reliability-focused assessment strategy and demonstrates that most of the investigated girders do not require intervention, even though considered inadequate, enhancing the efficiency and sustainability of infrastructure maintenance.

Keywords: reliability assessment, existing prestressed concrete I-girder bridges, Eurocode-based traffic load model, structural deterioration and damage.

1 Introduction

In recent years, assessing the structural safety of existing bridges has become increasingly critical due to ageing infrastructure and limited resources for their maintenance and replacement. The sustainability of existing structures passes through the possibility of lifetime extension, saving economic and environmental resources [1]. In the literature, methods and examples of reliability analysis of structures can be found, for example, in [2], [3] and [4]. Other studies adopt the reliability framework to consider additional knowledge about the structure, such as the updating of basic random variables or direct information on the probability of failure, such as proof loading of structures [5], [6], [7] and [8]. The JCSS Model Code [9] represents a valuable document for the reliability assessment of existing structural systems, such as [10] and [11]. However, full-probabilistic assessment of structures is not yet a widely adopted method, particularly for ordinary safety checks. Conventional verification methods, such as the Partial Safety Factor Method (PSFM) are widespread among the engineering community. However, results of this semi-probabilistic approach often indicate that certain elements are not verified according to the current design standards, imposing sometimes the necessity of expensive interventions or restrictions on serviceability. However, a valuable complementary alternative for evaluating the actual performance and residual capacity of existing structures is the reliability-based approach, which provides a more accurate assessment by explicitly considering uncertainties, enabling optimized decision-making, cost-effective interventions and improved risk management compared to traditional safety factor methods. Indeed, unlike traditional deterministic methods, reliability-based assessments can take into account all the types of uncertainties governing the problem, such as material and geometrical properties, load effects, model and statistical uncertainties and human error [12]. Moreover, reliability analysis provides a rational basis for eventually reducing the target reliability index based on considerations such as the reduced future service life and economic optimization, recognizing that existing structures have already endured a substantial portion of their design service life. Additionally, the higher costs associated with safety measures and retrofitting interventions on existing infrastructure, compared to new construction, further justify an accepted higher target probability of failure [13].

The focus of this paper is the analysis of the PC I-girder typology of existing bridges, whose fragility under traffic loads has been studied in [14] with Monte Carlo simulation.

2 Reliability Analysis

In a reliability analysis, different types and sources of uncertainties need to be considered. Specifically, in this paper, only physical and model uncertainties were considered to model the prior knowledge of material properties and structural models' prediction variability. The traffic load effect is based on Eurocode Load Model 1 [15] and its probabilistic definition. The estimated probability of failure refers to the prediction of the probability of failure of one single component of the whole structure (edge girder) for a specific time period, based on the hypothesis of invariance of random variables parameters and probabilistic model with time. The probability of failure is computed according to classical structural reliability theory, i.e. estimating the probability that a specific limit state LS_j, modelling a damage conditioning ξ_j, is exceeded in a fixed time period Δt.

$$P_f\left(LS_j, \Delta t, \xi_j\right) = P\left[LS_j(\Delta t, \xi_j) \leq 0\right] \qquad (1)$$

where the general expression of the limit state is

$$LS_j = \xi_j \theta_R R_j - \theta_E (G + TL(\Delta t)) \qquad (2)$$

with R_j the capacity associated with the failure mechanism j, G and TL the permanent and traffic load effects, θ_i the model uncertainty of the variable i.

In this study, First Order Reliability Method (FORM) was adopted, using the UqLab software [16] in MatLab environment [17]. In the following, the reliability index β is computed according to the well-known relationship $\mathrm{P_f} = \Phi(-\beta)$, with $\Phi(*)$ the cumulative distribution function (CDF) of the standard normal distribution.

2.1 Resistance

Flexure and shear at the Ultimate Limit State (ULS) were considered failure mechanisms. In particular, the ULS resisting bending moment M_R of the external PC girder was evaluated through the following simplified relationship:

$$M_R = 0{,}9\left(d_s \cdot A_s \cdot f_y + d_{sp} \cdot A_{sp} \cdot f_{p,01}\right) \qquad (3)$$

with A_s and A_{sp} the total reinforcement area of ordinary steel and prestressing steel, $0{,}9d_s$ and $0{,}9d_{sp}$ the reinforcement and prestressing steel lever arms, f_y and $f_{p,01}$ the yield strength of ordinary reinforcement and strands, respectively. Basic assumptions involve steel reinforcements lumped at its centroid, an elastic-perfectly plastic constitutive model for both ordinary and prestressing steel; concrete crushing in compression and yielded reinforcement due to the relatively low reinforcement ratio.

For the evaluation of the shear capacity, a more detailed consideration was required. Indeed, many bridges built with this construction typology in the second half of the 20th century—particularly in Italy—were typically designed within the elastic domain, relying primarily on the beneficial contribution provided by prestressing for shear resistance. As a matter of fact, quite often only minimal shear reinforcement is available, approximately three stirrups ($\phi 8$) per meter ($\rho_w \approx$ 0,7) fully anchored. This design approach results in low shear resistance when evaluated at the ULS using solely the truss model. Nevertheless, a pure elastic model is not completely adequate for ULS, where, in general, plastic reserves are expected to be available. Consequently, in the following, the shear capacity V_R of a PC girder was computed considering or not the presence of flexural cracking at the ULS. The shear-tension failure mode was assumed to be appropriate in sections where no flexure cracking occurs, according to Eurocode [18]:

$$V_{R,U} = \frac{I}{S} b_w \sqrt{f_{ct}^2 + f_{ct}\sigma_{cp}} \tag{4}$$

The analysis is conducted in the centroid of the cross-section, imposing that the mean principal tensile stress does not crack the beam web. The ratio between the inertia moment and static moment I/S was considered equal to $0{,}7d$ according to the Italian National Code [19].

When calculating internal shear force, the beneficial contributions of the residual prestressing force in the horizontal Eqn. (5) and vertical Eqn. (6) directions were taken into account.

$$P_x(x) = cos\big(\psi(x)\big)\,(1 - \Delta l)\sigma_{0p}A_{sp} \tag{5}$$

$$P_y(x) = sin\big(\psi(x)\big)\,(1 - \Delta l)\sigma_{0p}A_{sp} \tag{6}$$

where $\psi(x)$ is the equivalent-tendon slope to the horizontal at the distance x from the support, Δl the total instantaneous and long-term prestressing losses (in %), σ_{0p} the initial prestressing stress.

If the sections resulted to be cracked under bending moment, the truss model [18] was adopted, considering transversal reinforcement:

$$V_{R,T} = min\big(V_{R,S}; V_{R,C}\big) \tag{7}$$

The actual conditioned shear capacity of the section positioned at x from one of the supports $V_R(x)$ modelled can be described as:

$$V_R(x) = \begin{cases} V_{R,U} \; if \; M_D(ULS,x) < M_{CR}(x) \\ V_{R,T} \; if \; M_D(ULS,x) \geq M_{CR}(x) \end{cases} \tag{8}$$

With $M_D(ULS,x)$ the demand bending moment at the ULS in the section and M_{CR} the cracking bending moment considering construction stages.

In conclusion, considering that the shear failure and cracking are binary, i.e. the only two possible realizations are possible for each random variable, it is possible to solve the problem with the Total Probability Theorem assuming mutual exclusivity and collective exhaustivity of events.

2.2 Demand

The total demand load effect was considered as a combination of permanent and traffic load effects, apart from the beneficial prestressing load described in Eqn. (6). Uniformly distributed permanent load q_G acting on each girder was considered to model deck self-weight plus non-structural components. Uncertainties were related to weight density and dimensions of structural and non-structural members. According to the PMC (Joint Committee on Structural Safety, 2000), a Gaussian distribution can be assumed as random variable to model the permanent load effect G.

With regard to the traffic load effect, Eurocodes provide a comprehensive framework for bridge design and assessment in Europe. In particular, Load Model 1 (LM1) of [15] represents road and highway traffic loading models for design and assessment. For each section positioned at x from one of the supports and for the longitudinal position of the tandem load p_{TL}, LM1 allows the calculation of a characteristic value $Q_k^{LM1}(x, p_{TL})$, declared to represent an action effect with a return period of 1000 years, i.e. having a 5% probability of exceedance in 50 years assumed for that section and for that position of the load. Since this study did not have any available WIM data for the probabilistic characterization of the actual effects of traffic loads, the information on the return period was used to calibrate the distribution of maxima bending moment and shear effects on the edge girder for each section positioned at x from one of the supports and for each longitudinal position of the tandem load p_{TL} starting from the deterministic computation of $Q_k^{LM1}(x, p_{TL})$, filtered through Courbon-Engesser distribution factors for the considered deck cross-section.

Assuming that the Gumbel distribution is adequate for maxima effects and arbitrarily choosing a coefficient of variation CoV_{TL} for traffic load bending moment and shear, it is possible to calculate the parameters of the distribution considering that the characteristic value $Q_k^{LM1}(x, p_{TL})$ represents the k-th order quantile in a specific time period Δt. Considering $TL{\sim}Y$, whose realizations are y, the Probability (PDF) and Cumulative (CDF) Density Functions adopted for the Gumbel distribution with parameters (u,γ) are:

$$f_Y(y) = \gamma \exp\left[-\gamma(y-u) - e^{-\gamma(y-u)}\right] \tag{9}$$

$$F_Y(y) = \exp\left[-exp^{-\gamma(y-u)}\right] \tag{10}$$

The traffic random variable TL was obtained by solving the following linear system:

$$\begin{cases} k = \exp\left[-e^{-\gamma(Q_k^{LM1}-u)}\right] \\ CoV_{TL} = \dfrac{\sigma_Y}{\mu_Y} = f(\gamma, u) \end{cases} \tag{11}$$

Figure 1 and Figure 2 illustrate how for a generic traffic load effect $Q_k^{LM1}(x, p_{TL})$ and a fixed coefficient of variation CoV_{TL}, the probabilities of exceedance have to vary to be consistent with the 1000-yrs return period as a function of the reference period Δt, arbitrarily considered to be [1; 50; 100] years.

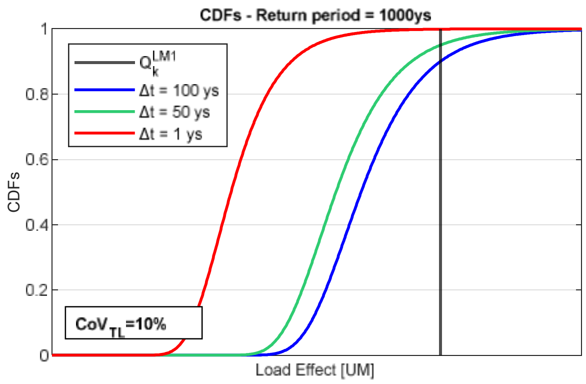

Figure 1. CDFs for three Δt

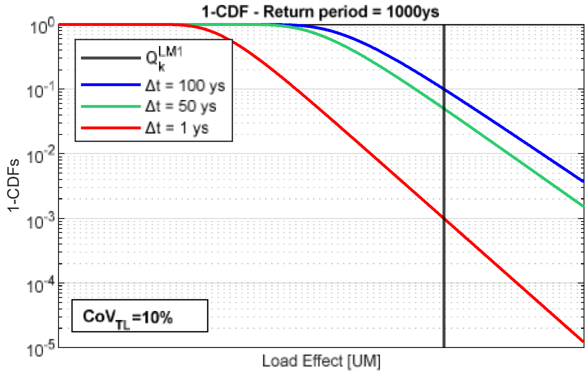

Figure 2. Exceeding probability for different Δt

2.3 Target Reliability

Defining target reliabilities is paramount for a reliability-based design and assessment of existing structures. Eurocode prescribes an annual reliability index for new structures up to 4,7. In Table 1 the suggested annual target reliability index from [9] for ULS are reported, based on cost-benefit analysis on a portfolio of structures.

Table 1. ULS target reliability indexes – JCSS [9]

	Consequences of failure		
Relative CSM*	Minor	Moderate	Large
Large (A)	*3,1*	***3,3***	***3,7***
Normal (B)	*3,7*	***4,2***	***4,4***
Small (C)	*4,2*	*4,4*	*4,7*

The target reliability index is based both on the consequences of failure, i.e. depending both on the ratio between total and reconstruction costs and on the type of failure and structure ductility reserves. It can be interpreted as the Consequences Class (CC) of Eurocode [20]. In general, depending on their importance and the network to which they belong, bridges are associated with large or moderate consequences of failure. The target values should also consider the relative Cost of Safety Measure (CSM), a synthetic parameter indicating the potential costs of interventions. For existing structures is suggested to accept higher values of the annual probability of failure since it is necessary to account for the higher costs of achieving a higher reliability, in accordance with [10], [12] and [13].

3 Case study

3.1 General description

A real case study was chosen to analyse the reliability of existing I-girder PC bridge typology. Built during the '60s and with a total length of 900 m with 21 spans, the viaduct is located along an important highway in Southern Italy. With a span length of 42 m, the bridge deck is simply supported and it is composed of 3 m high PC I-girders, a concrete top slab (variable thickness between 0,20 and 0,30 m) and four transverse prestressed concrete beams (Figure 3). Engesser-Courbon influence line was computed for the external girder (1) and distribution factors for the three lanes considered are displayed in Figure 3.

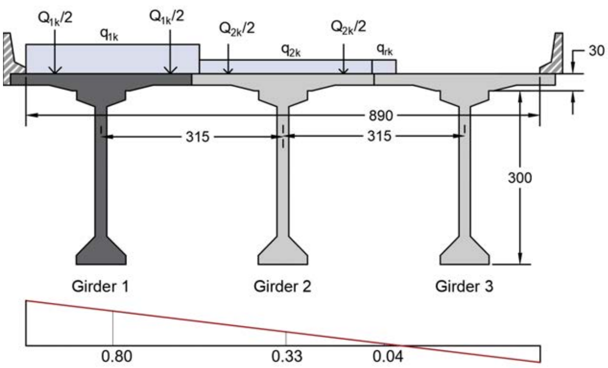

Figure 3. Deck cross-section, influence line and distribution factors (dimensions in cm)

Geometrical variables were considered deterministic and summarized in Table 2.

Table 2. Geometrical variables

Property	Symbol	Unit	Value
Span Length	L	m	42
Carriageway Width	w	m	8,9
Total Deck Height	H	m	3,3
Prestressing Steel ED*	d_s	mm	3260
Prestressing Steel Area	A_{sp}	mm^2	7740
Reinforcing Steel ED*	d_{sp}	mm	3135
Reinforcing Steel Area	A_s	mm^2	2670
Stirrups Area	A_{sw}	mm^2	100
Stirrups Distance	s	mm	290

*Effective Depth

3.2 Flexural damage modelling

Detailed visual inspections were conducted on edge girders of the viaduct, allowing for a detailed assessment of the structural condition of the elements. The analysis revealed a wide range of deterioration, particularly located at the bottom side of the edge beam near mid-span.

Data obtained from visual inspections regarding the deterioration state of the viaduct were considered to evaluate the reduction in flexure capacity of the edge beams at the mid-span through the parameter ξ_F, which values are based on the following facts.

Composed of 85 simply-supported girders, only 41 edge beams were inspected for detailed quantification of prestressing and reinforcement steel corrosion, a part of a widespread concrete cover spalling. In 13 beams, only a phenomenon of strand oxidation was identified, without any reduction of prestressing steel area. For this reason, they were excluded from the dataset. As regards the remaining 28 girders, in Figure 4 are reported the results of the data collected through the visual inspections and described through the parameters defined in the following.

The detected frequency of the number of Corroded Strands (NCS, Figure 4a) and frequency of the number of Broken Strands (NBS, Figure 4b) for each girder are reported. On average, two wires on seven were identified to be broken in corroded strands, while for broken condition all seven wires were detected to be broken by corrosion. Therefore, considering NS the total Number of Strands (80), the percentage of Total Lost Strands Area ($TLSA$, Figure 4c) was defined to reflect the overall loss of prestressing steel:

$$TLSA\,[\%] = \frac{1}{NS} \cdot \left[NBS + \frac{NCS}{7}\right]\% \qquad (12)$$

No information was available regarding the extent of reinforcement steel corrosion. However, its contribution remains low, accounting for approximately less than 10% of the global flexural strength in the undamaged cross-section. Therefore, including rebar corrosion, a global average flexural capacity reduction can be seen as the sum of the damage parameter $TLSA$ as regards the strands and an additional term on the degree of corrosion of reinforcing steel in the [0,10] % range. The worst condition inspected on a girder was associated with a total loss of prestressing steel, $NBS = 4$ and $NCS = 18$ ($TLSA = 8\%$), turning into a flexural capacity reduction of about 20%. Based on these results, the parameter ξ_F (see Eqn. (2)) for flexural capacity is fixed to have the following values:

$$\xi_F = [100 - 95 - 90 - 85 - 80]\% \qquad (13)$$

No assumptions were made regarding changes in mechanical properties due to deterioration, but only on the global variation in load-bearing capacity.

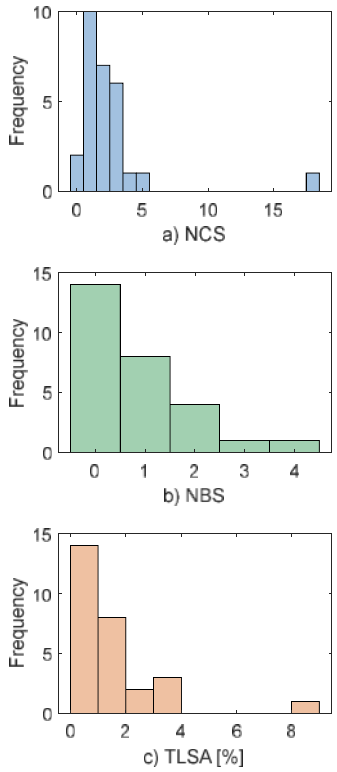

Figure 4. Deterioration parameters derived from visual inspections of the 28 considered girders: a) NCS; b) NBS; c) TLSA.

No signs of degradation or damage were reported near the support, where shear failure mode governs. For this reason, the shear reduction factor ξ_V was set to be equal to 1. Finally, inspection revealed no signs of deterioration of transversal girders.

3.3 Capacity-Demand Ratio

Considering the conventional Partial Safety Factor Method (PSFM), the Capacity-Demand-Ratio (CDR) can be evaluated as the ratio between design resistances and loads, obtained through the use of the so-called Partial Safety Factors (γ_i) (PSF) defined by national and international codes. PSF used in this paper are illustrated in Table 3 according to [19] and [20]:

Table 3. Partial Safety Factors

Symbol	Value	Object
γ_S	1,15	Steel
γ_C	1,50	Concrete
γ_G	1,35	Permanent Load
γ_{TL}	1,35	Traffic Load
γ_p	1,00	Prestressing

Capacity-Demand Ratios $CDR_j(\xi_j)$ were defined as the ratio between the design capacity and demand for the j-th failure mechanism considering the capacity reduction parameter ξ_j:

$$CDR_j(\xi_j) = \xi_j \cdot \frac{C_d}{D_d} \qquad (14)$$

The flexure $CDR_F(\xi_F)$, illustrated in Table 4, were evaluated only for the mid-span of the edge girder, i.e. $x = p_{TL} = L/2$.

Table 4. Mid-span Flexural CDR_F

ξ_F [%]	100	95	90	85	80
$CDR_F(\xi_F)$	1,09	1,04	0,98	0,93	0,88

Unlike for flexure, for shear the beam was discretized into 21 sections; for each of them at distance x from the support, resistance was computed according to Eqn. (8), while the characteristic load effect was determined as $V_k^{LM1}(x, p_{TL})$ assuming the tandem position p_{TL} to maximize the effect in that section. For this specific case and influence line, it was assumed $x \approx p_{TL}$, i.e., with an axle nearly aligned with the section. The lowest $CDR_V(\xi_V = 100\%)$ in shear along the beam was computed at a distance d from the support equal to 0,79.

3.4 Probabilistic modelling

3.4.1 Material properties

Material properties were defined on prior knowledge based on original design drawings. Only for concrete properties, in-situ concrete cores were available. Particularly, in Table 5 are illustrated the material properties modelled as random variables, whose main values were obtained from available documentation and CoV based on literature, such as [9].

Table 5. Material random variables

Symbol	Mean	Unit	CoV	RV Model
$f_{p,01}$	1645	MPa	2,5%	Normal
σ_{0p}	1355	MPa	3,0%	Normal
Δl	0,25	-	10,0%	Normal
f_y	500	MPa	6,0%	Normal
f_c	35,6	MPa	20%	Lognormal
f_{ct}	2,7	MPa	20%	Lognormal

In Table 5, $f_{p,01}$ is the conventional yielding strength of prestressing steel; f_y the yield strength of reinforcement steel; f_c and f_{ct} the concrete compressive and tensile strength.

3.4.2 Loads

To model deck self-weight and non-structural components, the mean value was assumed to be equal to the nominal value reported by original drawings confirmed by visual inspections, i.e. a uniformly distributed load $q_G = 52\ kN/m$. The coefficient of variation CoV_G was set equal to 5%.

As regards the traffic load effect, the transversal position of traffic loads and the relative distribution factors were assumed to be as in Figure 3. For the bending moment, the characteristic value at the mid-span was $M_k^{LM1} = 10{,}9\ kNm$. In Figure 5 three PDFs are plotted for the distributions modelling the annual ($\Delta t = 1yr$) maximum bending moment at the girder mid-span considering the characteristic value M_k^{LM1} for three values of $\mathrm{CoV_{TL}} = [5; 10; 15]\%$.

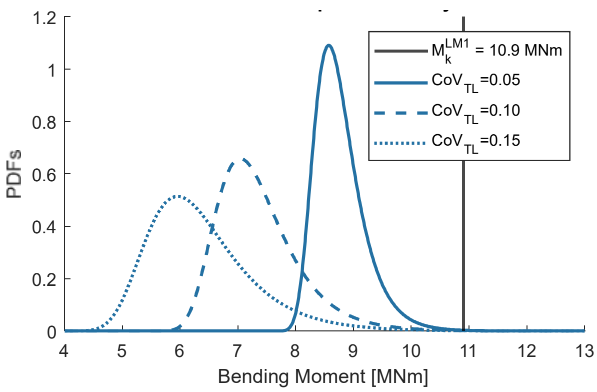

Figure 5. PDF of annual distribution of maximum bending moment at mid-span for three CoV_{TL}

With regard to shear, for each $V_k^{LM1}(x, p_{TL})$ three distributions of annual maxima were fitted for the three values of $\mathrm{CoV_{TL}}$ for each of the 21 sections.

3.4.3 Model uncertainties

In order to consider the difference between the capacity and load model predictions from the reality and experiments, model uncertainties were introduced and modelled as random variables, classified for the failure mechanism considered. Load model uncertainty was introduced due to the simplified method used for transversal distribution factors.

Table 6. Model Uncertainties

Symbol	Mean	CoV	Object	RV Model
$\theta_{R,F}$	1,00	0,05	Flexural Capacity	Lognormal
$\theta_{R,V}$	1,00	0,10	Shear Capacity	Lognormal
θ_E	1,00	0,10	Loads	Lognormal

3.5 Results

In this section, results of reliability analysis are presented, demonstrating that most of the sections under consideration would not require intervention for the flexural limit state. The analysis is based on a comparison between the computed annual β values and the corresponding β target depending on the consequence class assigned to the bridge.

3.5.1 Flexure Limit State

In Figure 6, the flexural annual reliability index β at the mid-span section is presented for five values of the resistance reduction parameter ξ_F in order to cover the overall residual capacity scenarios of the external girders affected by the corrosion.

The analysis performed on the bridge according to PSFM revealed CDR_F lower than unity in several cases, i.e. the values were depicted by the shaded area. In ordinary contexts, such results indicate potential structural vulnerabilities that may compromise bridge safety.

However, when considering the reliability-based analysis, i.e. at the distance between the reliability indexes and target reliability for existing structures

(3,7 and 3,3 for CC3 and CC2, respectively), sections with a CDR_F equal to 0,98 and 0,93 would not require any strengthening intervention. For the section with CDR_F equal to 0,88 corresponding to 20% capacity reduction, β is higher than 3,3, but additional information on traffic load could provide higher values than 3,7.

The potential significance of this result becomes even more evident when observing that almost all the beams in which deterioration was analysed are represented by CDR_F values of 1,04, 0,98 and 0,93, with only one beam at 0,88.

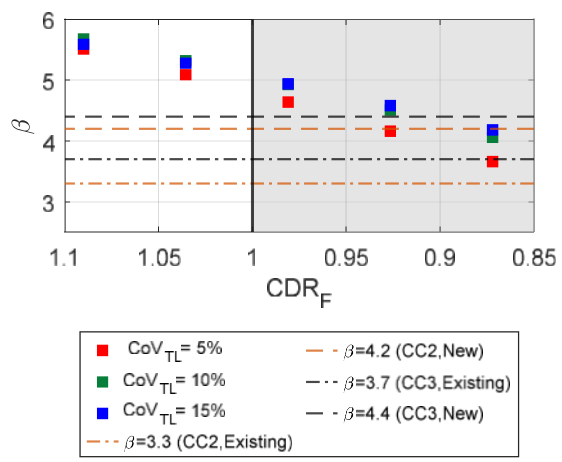

Figure 6. Values of β for flexure for three CoV_{TL} compared to CC3 and CC2 target reliabilities.

3.5.2 Shear Limit State

The beam was found to be unsafe according to PSFM, having the lowest CDR_V equal to 0,79. It is possible to extend the reasoning and the evidence discussed for bending to the shear ULS. First of all, considering d_{sp} the prestressing steel effective depth, the sections located at a distance $x < d_{sp}$ are not considered, according to code provisions accounting for arch action at supports.

In Figure 7, a part of the chosen CoV_{TL}, it is possible to observe how all sections along the beam (x/L) have a reliability index higher than the minimum target reliability for the existing structures , i.e. all the points are above $\beta_{CC3,existing}$. However, this is not straightforward for higher target reliability, such as for structures that are required to be code conforming with β_{new}. In this case, a few sections with $d_{sp}/L < x/L < 0{,}1$ require more attention.

Additionally, it is observed that the reliability index for shear in prestressed beams does not follow a monotonic trend increasing towards the midspan.

For the case study, the abrupt variation of β visible at $x/L = 0{,}35 - 0{,}38$ is due to the non existence of the beneficial vertical component induced by prestressing, as the strands layout is horizontal from this section to the mid-span. The influence of this variation is very significant on the overall reliability.

An additional feature is the variation of the reliability index trend at $x/L = 0{,}15$ due to the combination of a higher probability that the section is flexurally cracked and that the truss-model shear resistance is low, i.e. the conditional probability of shear failure considering the truss model is higher than that of the shear-tension model. This means that the former starts governing the shear capacity from $x/L = 0{,}15$. However, lower β values are achieved at shorter distance from the supports where the second model governs.

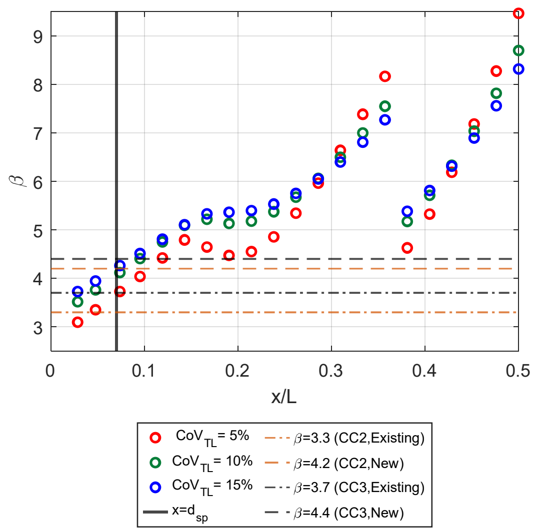

Figure 7. Values of β for shear for three CoV_{TL} compared to CC3 and CC2 target reliabilities.

4 Conclusions

The reliability analysis conducted in this study according to FORM demonstrates that most of the investigated edge girders would not require interventions both for bending moment and shear capacity, as their β consistently exceeds the target thresholds for existing structures. This approach and these results provide valuable insights into the safety assessment of PC I-girder bridges, allowing the optimization of retrofitting strategies and focusing the need of proof load testing or interventions only on critically vulnerable elements with very high consequences of failure, thereby enhancing the efficiency and sustainability of maintenance activities.

Acknowledgements

This study was developed within the CSLLP-ReLUIS project funded by the Italian High Council of Public Works.

5 References

[1] Diamantidis, D., Tanner, P., Holicky, M., O. Madsen, H., & Sykora, M. (2025). On reliability assessment of existing structures. Structural Safety; 113.

[2] Diamantidis, D. (1987). Reliability assessment of existing structures. Engineering Structures; 9:177-182.

[3] Ellingwood, B. R. (1996). Reliability-based condition assessment and LRFD for existing structures. Structural Safety; 18:67-80.

[4] Faber, M. H. (2000). Reliability-based assessment of existing structures. Progress in Structural Engineering and Materials; 2: 247-253.

[5] Hall, B. (1988). Reliability of service-proven structures. Journal of Structural Engineer; 114.

[6] Lin, T. S., & Nowak, A. S. (1984). Proof Loading and Structural Reliability. Reliability Engineering; 8: 85-100.

[7] Addonizio, G., de Vries, R., Lantsoght, E. O., & Losanno, D. (2024). Reliability of I-girder PC bridges through proof load testing: Preliminary results. Bridge Maintenance, Safety, Management, Digitalization and Sustainability. CRC Press, Page 9.

[8] de Vries, R., Lantsoght, E., Steenbergen, R., Hendriks, M., & M. Naaktgeboren. (2025). Structural reliability updating on the basis of proof load testing and monitoring data. Engineering Structures; 330.

[9] Joint Committee on Structural Safety. (2000). JCSS Probabilistic Model Code.

[10] Fédération Internationale du Béton (FIB). (2016). Bulletin 80 - Partial factor methods for existing concrete structures.

[11] European Commission, Joint Research Centre. (2024). Reliability background of the Eurocodes. Luxembourg: Publications Office of the European Union.

[12] Melchers, R., & Beck, A. (2017). Structural Reliability Analysis and Prediction. Wiley.

[13] Steenbergen, R., & Vrouwenvelder, A. (2010). Safety philosophy for existing structures and partial factors for traffic loads on bridges. HERON, 55.

[14] Miluccio, G., Losanno, D., Parisi, F., & Cosenza, E. (2023). Fragility analysis of existing prestressed concrete bridges under traffic load according to new Italian guidelines. Structural Concrete; 24:1053-1069.

[15] EN 1991-2 - Comité Européen de Normalisation. (2003). Eurocode 1: Actions on structures - Part 2: Traffic loads on bridges. Brussels.

[16] Marelli, S., & Sudret, B. (2014). UQLab: A Framework for Uncertainty Quantification in MATLAB. The 2nd International Conference on Vulnerability and Risk Analysis and Management, (pp. 2554-2563). Liverpool.

[17] The MathWorks Inc. (2023). MATLAB R2023b. Natick, Massachusetts.

[18] EN 1992-1-1 - Comité Européen de Normalisation. (2004). Eurocode 2: Design of concrete structures - Part 1-1: General rules and rules for buildings. Brussels.

[19] Italian Ministry of Infrastructures and Transportation. (2018). DM 17/01/2018. Aggiornamento delle "Norme tecniche per le costruzioni'. Rome, Italy.

[20] The European Union Per Regulation . (2002). EN 1990:2002 Eurocode - Basis of structural.